ORIGINAL PAPER

# Distinguishing breast cancer cells using surface-enhanced Raman scattering

Jing Yang · Zhuyuan Wang · Shenfei Zong ·
Chunyuan Song · Ruohu Zhang · Yiping Cui

**Abstract** The detection and identification of epidermal growth factor receptor 2 (HER2)-positive breast cancer cells is crucial for the clinic therapy of breast cancer. For the aim of the detection, a novel surface-enhanced Raman scattering (SERS) probe for distinguishing breast cancers at different HER2 statuses is reported in this paper. In such a probe, anti-HER2 antibody-conjugated silver nanoparticles have been synthesized for specific targeting of HER2-positive breast cancer cells. More importantly, different from the previously reported SERS probe for targeting cancer cells, *p*-mercaptobenzoic acid is utilized as both the Raman reporter and the conjugation agent for attaching antibody molecules, which leads to a much simplified structure. For investigating the ability of such a probe to distinguish breast cancer cells, SKBR3 and MCF7 cells were chosen as two model systems, which are HER2-positive- and HER2-negative-expressing cells, respectively. The experimental results reveal that SKBR3 cells exhibit much stronger SERS signals than MCF7 cells, indicating that the probe could be utilized to distinguish breast cancer cells at different HER2 statuses. This kind of SERS probe holds a potential for a direct detection of living breast cancer cells with the advantages of easy fabrication, high SERS sensitivity, and biocompatibility.

**Keywords** Surface-enhanced Raman scattering · HER2 · Cancer targeting · SKBR3 · MCF7

J. Yang · Z. Wang · S. Zong · C. Song · R. Zhang · Y. Cui (✉)
Advanced Photonics Center,
Southeast University,
Nanjing 210096, China
e-mail: cyp@seu.edu.cn

## Introduction

Overexpression of human epidermal growth factor receptor 2 (HER2), also known as a tyrosine kinase transmembrane receptor, has been found in various cancers including breast, ovarian, and lung cancers [1]. In the case of breast cancer, patients with a HER2-positive status are generally associated with a worse prognosis and a higher rate of disease recurrence compared with patients with a HER2-negative status [2]. HER2 is an important biomarker whose status plays a pivotal role in therapeutic decision making for breast cancer patients and in determining their clinical outcomes [3]. For example, Herceptin, an anti-breast cancer drug cleared by the US Food and Drug Administration, inhibits the growth of HER2-overproducing tumor cells and is well tolerated for HER2-positive breast cancer patients. However, Herceptin may cause cardiotoxicity for HER2-negative breast cancer patients [4]. Thus, identifying the HER2 status of breast cancer cells is of great clinical significance for breast cancer therapies. Currently, the most commonly used methods for assessing HER2 status are immunohisto-chemistry and fluorescence in situ hybridization [5]. These two methods suffer from several drawbacks such as being relatively time-consuming and not suitable for the direct detection of living cells or tissues.

Recently, surface-enhanced Raman scattering (SERS) has attracted considerable interest as a promising tool in bioanalysis due to its unique advantages such as resistance to photobleaching, narrow spectral bands, and low detection concentrations [6–9]. Up to this date, several SERS probes have been successfully demonstrated for targeting cancer cells [10–16], including HER2-positive cancer cells [10, 17–20]. For preparing SERS probes, Raman reporters are usually being introduced onto gold or silver nano-
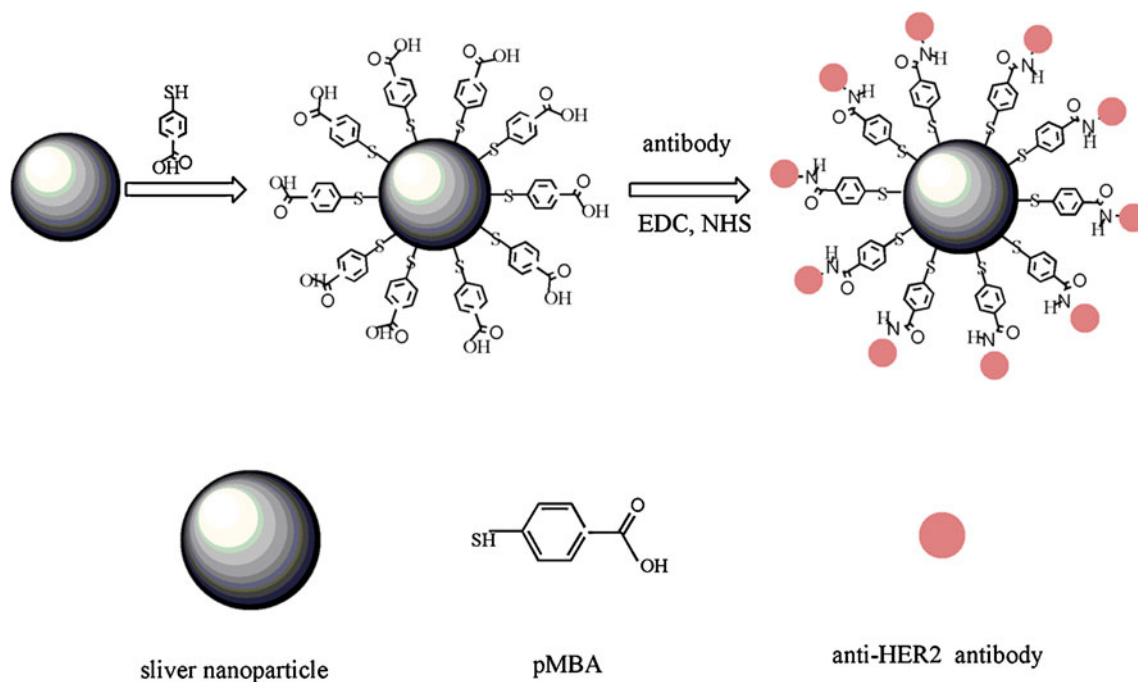
**Scheme 1** Schematic illustration of antibody-conjugated SERS probe synthesis

particles, and the outer surfaces of the probes are functionalized with the specific targeting biomolecules. Among the previously reported SERS probes for targeting cancer cells, the core/shell structure has been widely employed. For example, Jun et al. [14] successfully developed a multifunctional SERS probe for cancer cell targeting and separation in which a silica shell was utilized to coat the silver-embedded magnetic nanoparticles as well as to conjugate the antibody molecules. Wang et al. [16] demonstrated a SERS probe for detecting circulating tumor cells using thiolated polyethylene glycol to improve the stability of the probe.

Here, we develop a novel structure of SERS probe for distinguishing breast cancer cells at different HER2 statuses. In such a structure, $p$-mercaptobenzoic acid (pMBA) molecules are used as both the Raman reporter for generating SERS signals and the conjugation agent for attaching antibody molecules to silver nanoparticles. Specifically, pMBA grasps the silver nanoparticles through thiol groups and conjugates with antibodies by forming the stable amide bonds with the carboxyl groups. Thus, the fabrication process of such a SERS probe is straightforward because no shell is needed. For investigating the applications of the probe in targeting cancer cells, it was utilized to distinguish breast cancer cells at two different HER2 statuses: the HER2-positive SKBR3 cells and the HER2-negative MCF7 cells. The experimental results show that SKBR3 cells exhibit much stronger SERS signals than MCF7 cells, indicating that the SERS probe holds the

potential for distinguishing the HER2 status of different kinds of breast cancer cells.

## Experimental

### Materials

Mouse anti-HER2 monoclonal antibody was purchased from Fuzhou Maxim Biotech, Inc. Silver nitrate ($AgNO_3$) was obtained from Shanghai Shenbo Chemical Co., Ltd. Trisodium citrate dehydrate was purchased from Shanghai Heiwei Co., Ltd. pMBA was purchased from Sinopharm Chemical Reagent Co., Ltd. 1-Ethyl-3-[3-dimethy-lamino-propyl]carbodiimide hydrochloride (EDC) and $N$-hydrox-ysuccinimide (NHS) were purchased from Shanghai Jingchun Chemical reagent Co., Ltd. Water used in the experiments was ultrapure deionized water (resistance, 18 MΩ cm$^{-1}$).

### Silver nanoparticle preparation

The Ag nanoparticles were prepared as described by Lee and Meisel [21]. Briefly, $AgNO_3$ solution (50 mL, 10 mM) in 500 mL deionized water was boiled under continuous stirring. Then, 10 mL of 1% sodium citrate was added. The mixture was boiled with stirring for about 1 h. The final prepared Ag nanoparticles were greenish yellow in color; the nanoparticles were stored in the dark and aged for a
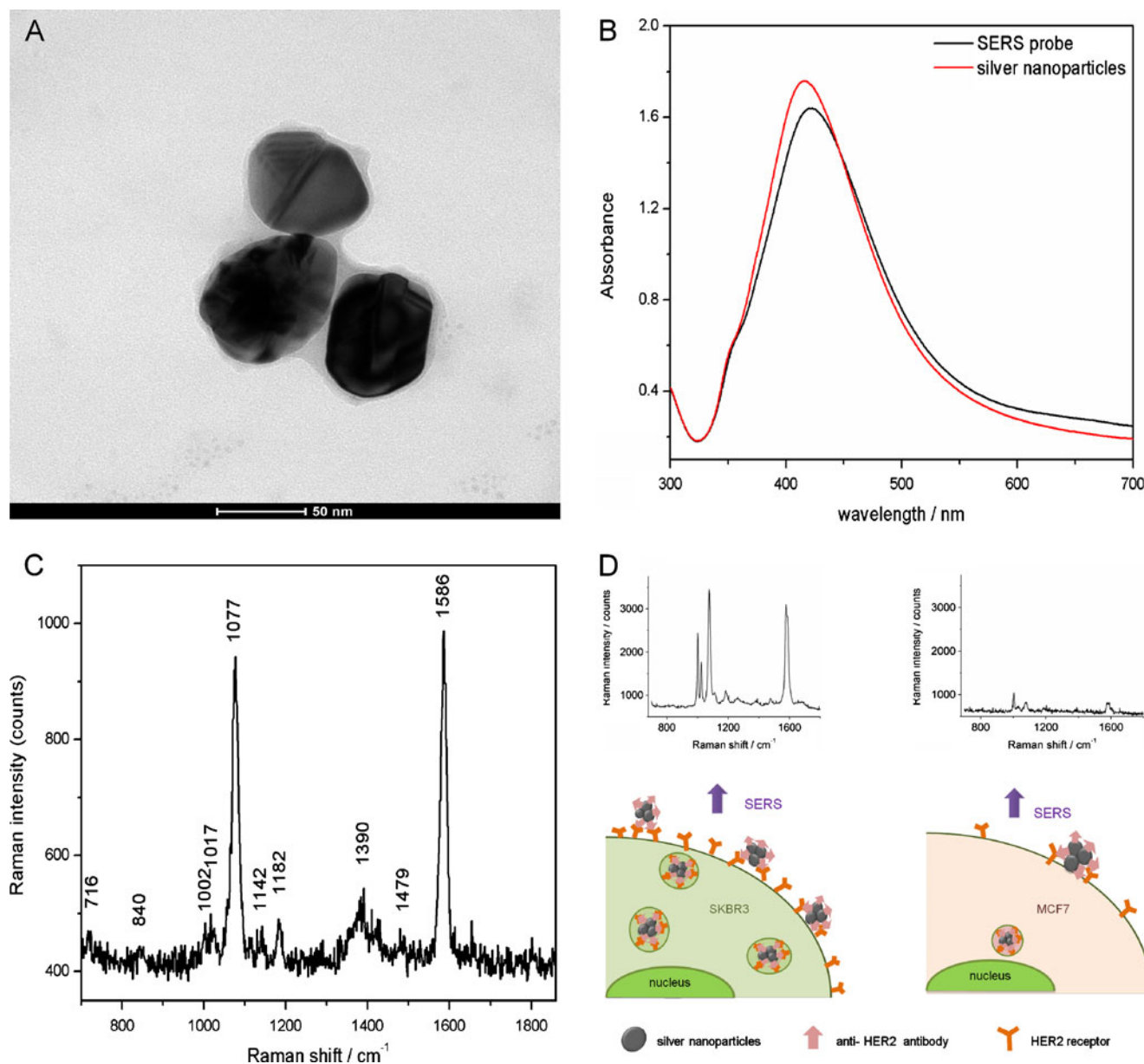
**Fig. 1** Transmission electron microscope image (**A**), extinction spectra (**B**), and SERS spectrum (**C**) of the SERS probe. **D** Illustration of cell targeting and SERS measurements

month. In this study, the Ag nanoparticles are from a single batch of colloid.

### Antibody-conjugated silver nanoprobe

A 10-mL solution of Ag nanoparticles was mixed with pMBA solution (100 μL, 1 mM in ethanol) and then stirred for 3 h. Afterwards, the solutions of EDC (50 μL, 10 mM) and NHS (12.5 μL, 100 mM) were added into the pMBA-coated silver nanoparticles. The carboxylic groups on the particle surfaces were activated to form reactive NHS ester intermediates. After 30 min of stirring, 10 μL of anti-HER2 monoclonal antibody was added into the carboxylic group-

activated silver nanoparticles and then stirred for another 4 h. The amine groups on the antibody molecules reacted with the active ester groups on the silver nanoparticle surfaces to form stable amide bonds. The antibody-conjugated silver nanoparticles were further purified by centrifugation at 6,000 rpm for 8 min. The supernatant solution was removed and the precipitated particles redispersed in 10 mL deionized water.

### Cell culture

SKBR3 breast cancer cells were purchased from the Cell Bank of Type Culture Collection of the Chinese Academy
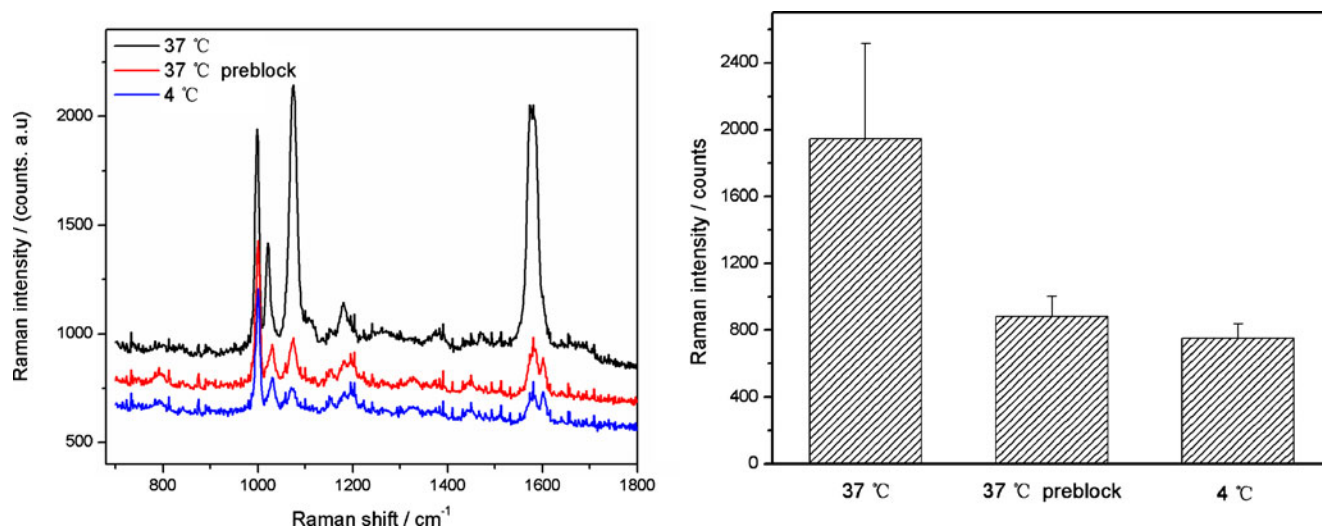
Fig. 2 *Left* SERS spectra of the probe in living SKBR3 cells under different conditions: incubated with nanoprobe for 4 h at 37 °C (*black*); incubated with the probe at 4 °C for 4 h (*blue*); and preblocked with free anti-HER2 antibody molecules for 2 h at 37 °C and then incubated with the nanoprobe for 4 h at 37 °C (*red*). *Right* SERS intensities of the bands at 1,077 cm$^{-1}$ correspond to the *left figure*

of Sciences. MCF7 breast cancer cells were purchased from Nanjing KeyGen Biotech. Co., Ltd. The SKBR3 and MCF7 cell lines were cultured in Dulbecco's modified Eagle's media and 1640 media, respectively, under a humidified atmosphere (5% $CO_2$ plus 95% air) at 37 °C. Media were supplemented with 10% fetal bovine serum (Biochrom) and 1% penicillin–streptomycin (Nanjing KeyGen Biotech. Co., Ltd.). In the proof-of-principle experiments, SKBR3 cells were seeded into tissue culture dishes (Corning) and incubated for 24 h; the culture medium was then replaced by a culture medium containing pMBA and antibody-conjugated SERS probe dispersion (3:1, *v/v*) and incubated under different conditions. One is that SKBR3 cells were

incubated with the probe for 4 h at 4 °C and another is that the SKBR3 cells were preblocked with free anti-HER2 monoclonal antibody molecules (10 μL) for 2h, and then, the above HER2 receptor-preblocked SKBR3 cells were incubated with the nanoprobe solution for 4 h at 37 °C. The other is that the SKBR3 cells were incubated with the probe for 4 h at 37 °C. To distinguish different breast cancer cells, SKBR3 cells and MCF7 cells were seeded into tissue culture dishes (Corning) and incubated for 24 h; the culture medium was then replaced by a culture medium containing pMBA and antibody-conjugated SERS probe dispersion (3:1, *v/v*) and incubated for 5 h at 37 °C. For each condition, one spectrum was collected in each cell, and the
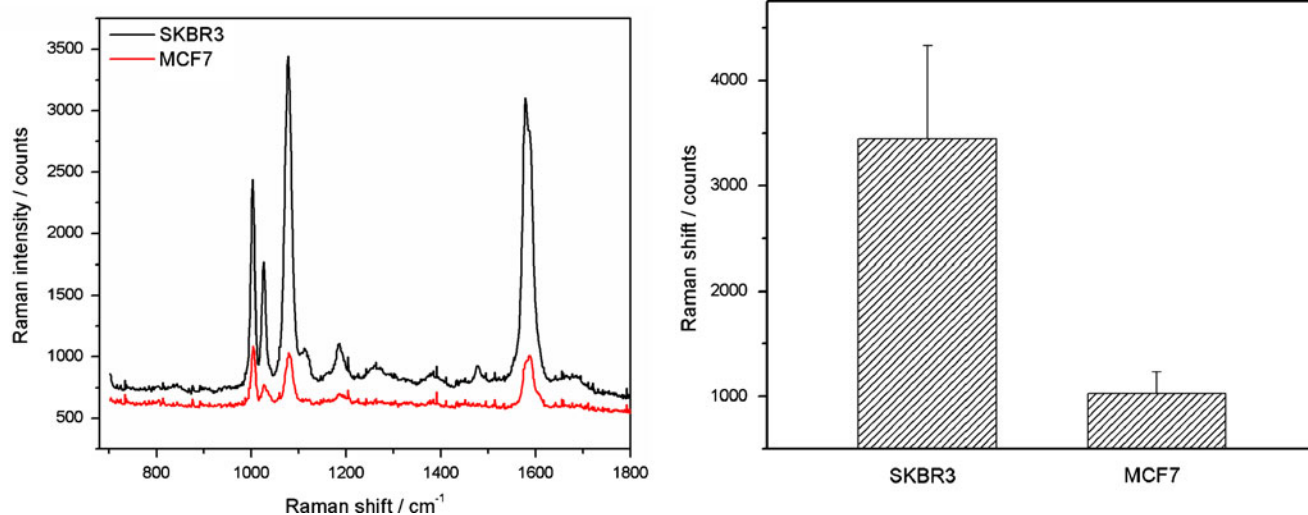


Fig. 3 *Left* SERS spectra of the probe in SKBR3 cells and in MCF7 cells. *Right* SERS intensities of the bands at 1,077 cm$^{-1}$ correspond to the left figure

**Fig. 4** Raman and bright light images of a single SKBR3 cell (**A**, **B**) and a single MCF7 cell (**C**, **D**)
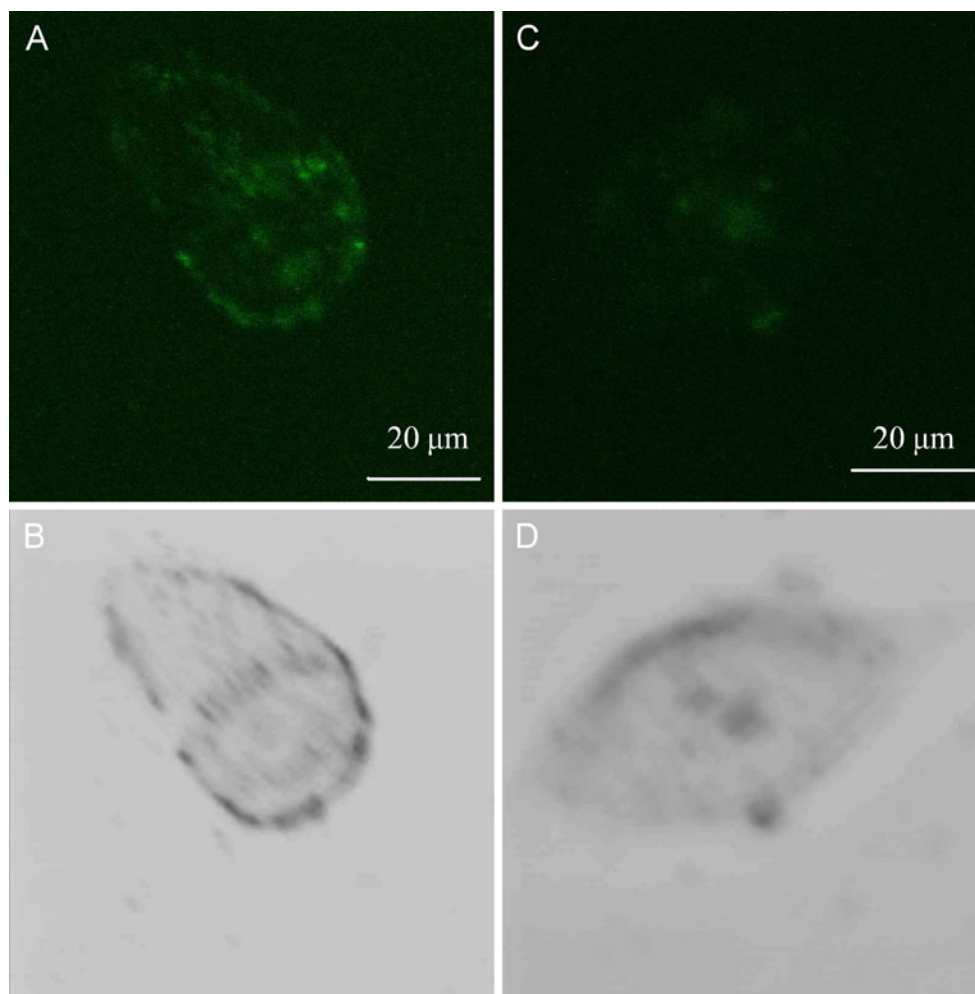


measured SERS spectra of 20 cells were used to obtain an average SERS spectrum. For fluorescent imaging, 20 μL of 1 mM Rhodamine 123 solution was added into SKBR3 cells and MCF7 cells pre-cultured with probe (1 mL probe solution to 3 mL culture medium) and without probe (3 mL culture medium), respectively, and incubated for 10 min at 37 °C. For Raman imaging, SKBR3 cells and MCF7 cells were cultured in the medium containing pMBA and antibody-conjugated SERS probe dispersion (3:1, $v/v$) for 5 h at 37 °C. Before SERS and fluorescent imaging experiments, the culture dishes were washed with PBS three times.

Instruments and measurement

Extinction spectra were collected using a Shimadzu model 3600 UV–vis NIR scanning spectrophotometer over the range from 300 to 700 nm. All the samples were loaded into a 1-cm quartz cell for measurements. Transmission electron microscopy (TEM) images characterizing the morphology of the SERS probe were obtained using a transmission electron microscope (Tecnai G2, Holland).

Fluorescent images were recorded by confocal microscopy with a ×10 microscope objective. The SERS spectra were measured at 632.8 nm excitation (2.3 mW at the sample), and Rayleigh scattering light was removed by a holographic notch filter. The Raman scattering light was recorded with a ×10 microscope objective and directed to an Andor shamrock spectrograph equipped with CCD. All SERS spectra reported here were the results of a single 30-s accumulation.

## Results and discussion

As illustrated in Scheme 1, unlike previous SERS probes based on core/shell structures, our SERS probe uses pMBA molecules as a bridge to link silver nanoparticles and antibody molecules, resulting in a much simplified structure. In the previous reports, pMBA has been widely used as a SERS reporter [22–25] due to its strong affinity to the surfaces of silver nanoparticles and strong SERS signals. In our presented SERS probes, pMBA molecules play a dual role as the Raman reporter and the conjugation agent, with
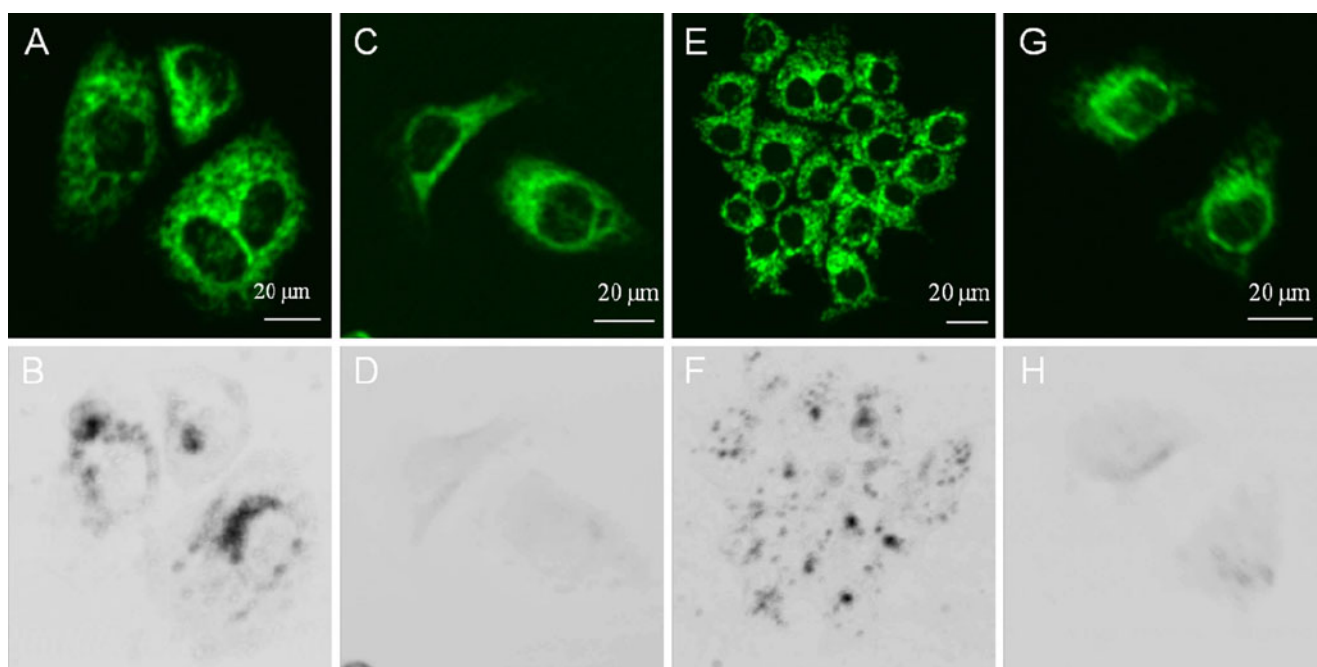
**Fig. 5** Fluorescent and bright light images of the SKBR3 (**A**, **B**) and MCF7 (**E**, **F**) cells after being incubated with the probe for 48 h and then stained with Rhodamine 123. SKBR3 (**C**, **D**) and MCF7 (**G**, **H**) cells without the probe were stained with Rhodamine 123 as controls

their thiol groups linking to the surfaces of silver nanoparticles and the carboxyl groups interacting with the amino groups of the antibody molecules. The carboxyl groups of the pMBA molecules can form stable amide bonds with the antibody molecules under the participation of EDC and NHS. Since it is not necessary to use the core/shell structure to separate the layer of Raman reporters from that of the targeting molecules, the fabrication protocol is simplified and straightforward, which is very important for improving the stability and reproducibility of a probe.

To prepare the SERS probe, silver nanoparticles with an average diameter of about 50 nm were synthesized as the Raman enhancement substrate, as shown in the TEM image (Fig. 1A). These silver nanoparticles were then functionalized with pMBA molecules to introduce carboxyl groups for conjugating with antibodies through amide reactions. The successful conjugation of antibody molecules to the surfaces of silver nanoparticles was confirmed by the thin film (a few nanometers) formed on the surfaces of silver nanoparticles. The extinction spectra of the pure silver nanoparticles and the antibody-conjugated SERS probe were shown in Fig. 1B. The spectrum of the pure silver nanoparticles showed a maximum absorption at 416 nm due to plasmon resonance. The antibody-conjugated SERS probe showed a slight decrease of the maximum absorption peak and a red shift of ~4 nm. By disturbing the citrate layers of the silver nanoparticles, the antibody conjugation process may lead to a slight aggregation, which is responsible for the decrease and red shift of the surface

plasmon resonance band [26]. As reported previously, the slight aggregation provides "hot spots" between silver nanoparticles, which can increase the Raman signals of the molecules adsorbed on the surfaces of silver or gold nanoparticles [27, 28]. Moreover, our experimental results show that the sight aggregates of silver nanoparticles can be successfully internalized by living cells.

Figure 1C shows the SERS spectrum of the antibody-conjugated SERS probe. The assignments of the Raman modes for pMBA have been studied previously [23, 29]. The most prominent Raman modes of pMBA are the modes at 1,077 and 1,586 cm$^{-1}$, assigned to the ring breathing and axial deformation modes of pMBA, respectively. The prepared antibody-conjugated SERS probe was further applied to in vitro studies.

In order to investigate how the antibody-conjugated SERS probe can be internalized within HER2-overexpressing cells, a competitive inhibition assay and a low-temperature assay were performed. In these assays, the breast cancer cell line SKBR3, expressing high levels of HER2 receptors on the cell membranes, was used as model cells. SKBR3 cells were incubated with the probe under three different conditions: (1) incubated with the probe for 4 h at 37 °C; (2) preblocked with free anti-HER2 antibody for 2 h and then incubated with the probe for 4 h at 37 °C, as a competitive inhibition assay; and (3) incubated with the probe for 4 h at 4 °C as a low-temperature assay. The experimental results are shown in Fig. 2. It can be observed that a stronger SERS signal was detected in the cells

incubated with the probe at 37 °C than in the cells incubated with the probe at 4 °C and those preblocked with free anti-HER2 antibody. The results indicate that more probe nanoparticles were internalized into SKBR3 cells under condition (1) than under conditions (2) and (3).

Receptor-mediated endocytosis is a process of specific identification in which the cells internalize nanoparticles through the inward budding of plasma membrane vesicles containing proteins with receptor sites specific to the molecules being internalized, as shown in Fig. 1D. In our experiments, the distinct suppression effect observed in the cells preblocked with the free anti-HER2 antibody indicates that the uptake of the SERS probe is a HER2 receptor-specific process. In addition, the receptor-mediated endocytosis is energy- and temperature-dependent. A low temperature might slow down the ligand–receptor binding rate and lead to a decrease of the internalization of nanoparticles. The decreased internalization amount of the probe at 4 °C compared with that at 37 °C demonstrates that the uptake of the probe by SKBR3 cells is an energy- and temperature-dependent process. All of the above results indicate that the SERS probe enters the SKBR3 cells through a receptor-mediated endocytosis mechanism.

Finally, to validate the applicability of the SERS probe in distinguishing breast cancer cells at different HER2 statuses, two breast cancer cells—SKBR3 cells and MCF7 cells—were chosen as model systems for the specific targeting of surface receptors. SKBR3 cells have abundant HER2 receptors on their surfaces, whereas MCF7 cells express HER2 only on a moderate level [30, 31]. The two cells were incubated with the SERS probe under the same condition. Figure 3 shows the SERS spectra of the probe after being incubated in SKBR3 cells and MCF7 cells for 5 h. The antibody-conjugated SERS probe showed a strong targeting effect. The SERS intensities of SKBR3 cells were about three to fourfold more than that of MCF7 cells. Raman images of single SKBR3 cell and MCF7 cell, as shown in Fig. 4, exhibit more SERS probe targets to SKBR3 cell than that of MCF7 cell. The results indicate that the antibody-conjugated SERS probe can sensitively target the SKBR3 cells, which can be utilized to test the HER2 status of breast cancer cells as well as to distinguish breast cancer cells.

To verify the biocompatibility of the SERS probe, cell proliferation was investigated using long-term fluorescence image. In brief, the two breast cancer cells—SKBR3 cells and MCF7 cells—were incubated with the SERS probe for 48 h at a high concentration as 1 mL probe solution to 3 mL culture medium. Then, the cells were stained with Rhodamine 123, a cell-permeant laser dye especially sequestered by active mitochondria [32, 33]. The Rhodamine 123-stained SKBR3 cells and MCF7 cells showed good morphology after a long incubation time with the probe,

as shown in Fig. 5. Interestingly, both cell lines continued to grow and divide after they took up a large number of the probe nanoparticles. The results indicate that the SERS probe does not show acute cytotoxicity at a rather high concentration with an incubation time as long as 48 h.

## Conclusions

A novel method based on SERS was developed for targeting HER2-positive breast cancer cells using a SERS probe with a simple structure. Such a method has the advantages of easy fabrication, rapid measurement, and high sensitivity for targeting HER2-overexpressed breast cancer cells. Experimental results show that the SERS probe is internalized into SKBR3 cells by a specific receptor-mediated endocytosis. SKBR3 cells exhibited much stronger SERS signals than MCF7 cells after being incubated with the SERS probe under the same condition. The obvious difference of SERS intensity detected from the two kinds of cells can be utilized to distinguish the different HER2 statuses of breast cancer cells. Long time incubation of the SERS probe with cells indicates that this SERS probe has good biocompatibility. Besides, by being conjugated with other proper biomolecular targeting ligands instead of an anti-HER2 antibody, this structure of SERS probe could be applied to target other kinds of cancer cells with high specificity and affinity.

## References

1. Miyano T, Wijagkanalan W, Kawakami S, Yamashita F, Hashida M (2010) Anionic amino acid dendrimer–trastuzumab conjugates for specific internalization in HER2-positive cancer cells. Mol Pharm 7(4):1318–1327. doi:10.1021/mp100105c
2. Hayes DF, Yamauchi H, Stearns V (2001) When is a tumor marker ready for prime time? A case study of c-erbB-2 as a predictive factor in breast cancer. J Clin Oncol 19(8):2334–2356
3. Xiao Y, Gao XG, Maragh S, Telford WG, Tona A (2009) Cell lines as candidate reference materials for quality control of ERBB2 amplification and expression assays in breast cancer. Clin Chem 55(7):1307–1315. doi:10.1373/clinchem.2008.120576
4. Hayes DF, Picard MH (2006) Heart of darkness: the downside of trastuzumab. J Clin Oncol 24(25):4056–4058. doi:10.1200/Jco.2006.07.5143
5. Jimenez RE, Wallis T, Tabasczka P, Visscher DW (2000) Determination of Her-2/neu status in breast carcinoma: comparative analysis of immunohistochemistry and fluorescent in situ hybridization. Mod Pathol 13(1):37–45
6. Kneipp J, Kneipp H, Kneipp K (2008) SERS—a single-molecule and nanoscale tool for bioanalytics. Chem Soc Rev 37(5):1052–1060. doi:10.1039/B708459p

7. Porter MD, Lipert RJ, Siperko LM, Wang G, Narayanana R (2008) SERS as a bioassay platform: fundamentals, design, and applications. Chem Soc Rev 37(5):1001–1011. doi:10.1039/B708461g

8. Charan S, Chien FC, Singh N, Kuo CW, Chen PL (2011) Development of lipid targeting raman probes for in vivo imaging of *Caenorhabditis elegans*. Chem A Eur J 17(18):5164–5169. doi:10.1002/chem.201002896

9. Doering WE, Nie SM (2002) Single-molecule and single-nanoparticle SERS: examining the roles of surface active sites and chemical enhancement. J Phys Chem B 106(2):311–317. doi:10.1021/Jp011730b

10. Kim JH, Kim JS, Choi H, Lee SM, Jun BH, Yu KN, Kuk E, Kim YK, Jeong DH, Cho MH, Lee YS (2006) Nanoparticle probes with surface enhanced Raman spectroscopic tags for cellular cancer targeting. Anal Chem 78(19):6967–6973. doi:10.1021/Ac0607663

11. Lee S, Kim S, Choo J, Shin SY, Lee YH, Choi HY, Ha SH, Kang KH, Oh CH (2007) Biological imaging of HEK293 cells expressing PLC gamma 1 using surface-enhanced raman microscopy. Anal Chem 79(3):916–922. doi:10.1021/ac061246a

12. Yang J, Wang ZY, Tan XB, Li J, Song CY, Zhang RH, Cui YP (2010) A straightforward route to the synthesis of a surface-enhanced Raman scattering probe for targeting transferrin receptor-overexpressed cells. Nanotechnology 21(34):345101. doi:10.1088/0957-4484/21/34/345101

13. Qian XM, Peng XH, Ansari DO, Yin-Goen Q, Chen GZ, Shin DM, Yang L, Young AN, Wang MD, Nie SM (2008) In vivo tumor targeting and spectroscopic detection with surface-enhanced Raman nanoparticle tags. Nat Biotechnol 26(1):83–90. doi:10.1038/nbt.1377

14. Jun BH, Noh MS, Kim J, Kim G, Kang H, Kim MS, Seo YT, Baek J, Kim JH, Park J, Kim S, Kim YK, Hyeon T, Cho MH, Jeong DH, Lee YS (2010) Multifunctional silver-embedded magnetic nanoparticles as SERS nanoprobes and their applications. Small 6(1):119–125. doi:10.1002/smll.200901459

15. Wang ZY, Zong SF, Yang J, Li J, Cui YP (2011) Dual-mode probe based on mesoporous silica coated gold nanorods for targeting cancer cells. Biosens Bioelectron 26(6):2883–2889. doi:10.1016/j.bios.2010.11.032

16. Wang X, Qian XM, Beitler JJ, Chen ZG, Khuri FR, Lewis MM, Shin HJC, Nie SM, Shin DM (2011) Detection of circulating tumor cells in human peripheral blood using surface-enhanced raman scattering nanoparticles. Cancer Res 71(5):1526–1532. doi:10.1158/0008-5472.Can-10-3069

17. Sha MY, Xu HX, Natan MJ, Cromer R (2008) Surface-enhanced Raman scattering tags for rapid and homogeneous detection of circulating tumor cells in the presence of human whole blood. J Am Chem Soc 130(51):17214. doi:10.1021/ja804494m

18. Maiti KK, Dinish US, Fu CY, Lee JJ, Soh KS, Yun SW, Bhuvaneswari R, Olivo M, Chang YT (2010) Development of biocompatible SERS nanotag with increased stability by chemisorption of reporter molecule for in vivo cancer detection. Biosens Bioelectron 26(2):398–403. doi:10.1016/j.bios.2010.07.123

19. Lee S, Chon H, Lee M, Choo J, Shin SY, Lee YH, Rhyu IJ, Son SW, Oh CH (2009) Surface-enhanced Raman scattering imaging of HER2 cancer markers overexpressed in single MCF7 cells

20. Park H, Lee S, Chen L, Lee EK, Shin SY, Lee YH, Son SW, Oh CH, Song JM, Kang SH, Choo J (2009) SERS imaging of HER2-overexpressed MCF7 cells using antibody-conjugated gold nanorods. Phys Chem Chem Phys 11(34):7444–7449. doi:10.1039/B904592a

21. Lee PC, Meisel D (1982) Adsorption and surface-enhanced Raman of dyes on silver and gold sols. J Phys Chem 86(17):3391–3395

22. Song CY, Wang ZY, Zhang RH, Yang J, Tan XB, Cui YP (2009) Highly sensitive immunoassay based on Raman reporter-labeled immuno-Au aggregates and SERS-active immune substrate. Biosens Bioelectron 25(4):826–831. doi:10.1016/j.bios.2009.08.035

23. Bishnoi SW, Rozell CJ, Levin CS, Gheith MK, Johnson BR, Johnson DH, Halas NJ (2006) All-optical nanoscale pH meter. Nano Lett 6(8):1687–1692

24. Talley CE, Jusinski L, Hollars CW, Lane SM, Huser T (2004) Intracellular pH sensors based on surface-enhanced Raman scattering. Anal Chem 76(23):7064–7068. doi:10.1021/ac049093j

25. Tan XB, Wang ZY, Yang J, Song CY, Zhang RH, Cui YP (2009) Polyvinylpyrrolidone–(PVP-) coated silver aggregates for high performance surface-enhanced Raman scattering in living cells. Nanotechnology 20(44):445102. doi:10.1088/0957-4484/20/44/445102

26. Felidj N, Aubard J, Levi G (1998) New approaches in the characterization of surface-enhanced Raman scattering-active substrates. J Raman Spectrosc 29(8):651–664

27. Schwartzberg AM, Grant CD, Wolcott A, Talley CE, Huser TR, Bogomolni R, Zhang JZ (2004) Unique gold nanoparticle aggregates as a highly active surface-enhanced Raman scattering substrate. J Phys Chem B 108(50):19191–19197. doi:10.1021/Jp048430p

28. Camargo PHC, Au L, Rycenga M, Li WY, Xia YN (2010) Measuring the SERS enhancement factors of dimers with different structures constructed from silver nanocubes. Chem Phys Lett 484(4–6):304–308. doi:10.1016/j.cplett.2009.12.002

29. Michota A, Bukowska J (2003) Surface-enhanced Raman scattering (SERS) of 4-mercaptobenzoic acid on silver and gold substrates. J Raman Spectrosc 34(1):21–25. doi:10.1002/jrs.928

30. Mojtahedi Z, Safaei A, Yousefi Z, Ghaderi A (2011) Immuno-proteomics of HER2-positive and HER2-negative breast cancer patients with positive lymph nodes. Omics 15(6):409–418. doi:10.1089/omi.2010.0131

31. Menendez JA, Vazquez-Martin A, Colomer R, Brunet J, Carrasco-Pancorbo A, Garcia-Villalba R, Fernandez-Gutierrez A, Segura-Carretero A (2007) Olive oil's bitter principle reverses acquired autoresistance to trastuzumab (Herceptin (TM)) in HER2-overexpressing breast cancer cells. BMC Cancer 7:80. doi:10.1186/1471-2407-7-80

32. Kirischuk S, Neuhaus J, Verkhratsky A, Kettenmann H (1995) Preferential localization of active mitochondria in-process tips of immature retinal oligodendrocytes. Neuroreport 6(5):737–741

33. Barnett DK, Kimura J, Bavister BD (1996) Translocation of active mitochondria during hamster preimplantation embryo development studied by confocal laser scanning microscopy. Dev Dyn 205(1):64–72